Steady-State $[Ca^{2+}]_i$-Force Relationship in Intact Twitching Cardiac Muscle: Direct Evidence for Modulation by Isoproterenol and EMD 53998

L. E. Dobrunz,* P. H. Backx,‡ and D. T. Yue*
*Department of Biomedical Engineering, The Johns Hopkins University School of Medicine, Baltimore, Maryland 21205 USA; and
‡Department of Medicine, University of Toronto, Toronto, Ontario M5G 2C4 Canada

ABSTRACT We have developed a novel method for measuring steady-state force-$[Ca^{2+}]_i$ relations in isolated, membrane-intact rat trabeculae that are microinjected with Fura-2 salt. Twitches are markedly slowed after inhibition of phasic Ca^{2+} release and uptake from the sarcoplasmic reticulum by addition of cyclopiazonic acid and ryanodine. During relaxation of slowed twitches, force and $[Ca^{2+}]_i$ trace a common trajectory in plots of force versus $[Ca^{2+}]_i$, despite very different histories of contraction. The common trajectory thereby provides a high resolution determination of the steady-state relation between force and $[Ca^{2+}]_i$. Using this method, we show that 1 μM isoproterenol, a β-adrenergic agonist, causes a rightward shift (Hill function $K_{1/2}$ increased from 0.39 ± 0.07 μM to 0.82 ± 0.23 μM, $p < 0.02$, $n = 6$) and a decreased slope (n_H decreased from 5.4 ± 1.1 to 4.0 ± 1.4, $p < 0.02$) of the steady-state force-$[Ca^{2+}]_i$ curve, with no change in maximal force (F_{max} = 99.2 ± 2.2% of control). In contrast, 2 μM EMD 53998, a racemic thiadiazinone derivative, causes a leftward shift ($K_{1/2}$ decreased from 0.42 ± 0.02 μM to 0.30 ± 0.06 μM, $p < 0.02$, $n = 4$) with no change in slope of the steady-state force-$[Ca^{2+}]_i$ curve, accompanied by a modest increase in maximal force (F_{max} = 107.1 ± 4.6% of control, $p < 0.02$). To gain mechanistic insight into these modulatory events, we developed a simple model of cooperative thin filament activation that predicts steady-state force-$[Ca^{2+}]_i$ relationships. Model analysis suggests that isoproterenol decreases cooperativity arising from nearest-neighbor interactions between regulatory units on the thin filament, without change in the equilibrium constant for Ca^{2+} binding. In contrast, the effects of EMD 53998 are consistent with an increase in the affinity of strong-binding cross-bridges, without change in either the affinity of troponin C for Ca^{2+} or cooperative interactions.

INTRODUCTION

The transduction of a transient rise in cytosolic calcium concentration ($[Ca^{2+}]_i$) into force and/or shortening is the fundamental basis of cardiac contraction. Changing the myofilament sensitivity to activator calcium is therefore a key potential mechanism for physiological and pharmacological regulation of cardiac performance.

One salient example of physiological control concerns β-adrenergic stimulation, which is known to increase the strength of contraction and to accelerate the rate of relaxation (see Tsien, 1977, for review). Because β-adrenergic stimulation also increases heart rate (Akahane et al., 1989), the faster rate of force decline is critical to allow for complete relaxation between beats. This accelerated relaxation is caused in part by an increased uptake rate of activator calcium into the sarcoplasmic reticulum (SR) (Tada and Katz, 1982). Another proposed mechanism for the faster rate of force relaxation is an enhanced Ca^{2+} off-rate from troponin C, as inferred from a rightward shift in the steady-state force-pCa ($-\log_{10}([Ca^{2+}]_i)$) curve measured in skinned muscle (Puceat et al., 1990).

Apart from physiological control mechanisms, new classes of pharmacological interventions may directly influence cardiac contraction through alterations in the myofilament sensitivity to $[Ca^{2+}]_i$. Among these interesting agents is EMD 53998 (EMD), a racemic thiadiazinone derivative that has been reported to sensitize myofilaments to $[Ca^{2+}]_i$, as evidenced by a leftward shift of the force-pCa relationship in skinned muscle (Beier et al., 1991). An increase in myofilament sensitivity would produce an increase in developed tension without necessitating an increase in $[Ca^{2+}]_i$.

Although suggestive, the evidence for physiologically and pharmacologically pertinent modulation of myofilament sensitivity, obtained mainly from skinned cardiac muscle preparations, remains indirect. Large differences may be found between steady-state relationships determined in skinned versus intact muscle (Yue et al., 1986; Gao et al., 1994). This discrepancy makes it imperative to establish the proposed sensitization or desensitization of myofilaments to $[Ca^{2+}]_i$ in intact muscle. Yet this is difficult to demonstrate because force and calcium are normally changing rapidly relative to each other, precluding determination of a steady-state relationship.

One approach for estimating steady-state relationships in intact preparations uses tetanic contractions to produce a quasi-steady state between force and $[Ca^{2+}]_i$. With aequorin as an indicator to estimate $[Ca^{2+}]_i$, Okazaki et al. (1990) used tetani to argue that isoprenaline, a β-adrenergic agonist, desensitizes myofilaments to $[Ca^{2+}]_i$ in intact muscle. However, Yue et al. (1986) demonstrated the existence of oscillations of both force and $[Ca^{2+}]_i$ during tetanic contraction at submaximal levels

Received for publication 11 August 1994 and in final form 11 April 1995.
Address reprint requests to D. T. Yue, Department of Biomedical Engineering, The Johns Hopkins University School of Medicine, 713 Ross Bldg., 720 Rutland Ave., Baltimore, MD 21205. Fax: 410-955-0549; E-mail: dyue@bme.jhu.edu.

0006-3495/95/07/189/13 $2.00

of activation. Thus there may be spatial gradients of activation within the muscle, thereby rendering it difficult to interpret results of this kind.

To overcome these limitations, we have developed a new technique for measuring steady-state force-$[Ca^{2+}]_i$ relationships in intact cardiac muscle. We measured force and calcium concentration in rat trabeculae during relaxation of twitches that were dramatically slowed by disabling the SR with cyclopiazonic acid (CPA), an agent that inhibits the SR Ca^{2+}-ATPase (Seidler et al., 1989), and ryanodine, a plant alkaloid that blocks release of Ca^{2+} from the SR (Sutko et al., 1985). $[Ca^{2+}]_i$ was measured using Fura-2 salt, a fluorescent Ca^{2+}-sensitive dye that was loaded into the muscle by iontophoresis (Backx and ter Keurs, 1993). This provides uniform loading of the entire muscle, thus avoiding one of the major problems of aequorin.

We find that force and $[Ca^{2+}]_i$ are both slowed to such a great extent that they effectively reach steady state during relaxation, as manifested by a unique relationship between force and $[Ca^{2+}]_i$ that is independent of the history of contraction. This unique force-$[Ca^{2+}]_i$ trajectory yields an in vivo steady-state force-$[Ca^{2+}]_i$ relationship. We use this technique to show that in intact twitching cardiac muscle, isoproterenol causes a pronounced rightward shift, and EMD 53998 induces a clear leftward shift in the force-$[Ca^{2+}]_i$ relationship. These results provide the clearest evidence yet for physiological and pharmacological modulation of myofilament sensitivity to $[Ca^{2+}]_i$ in intact muscle. Preliminary reports of this work have appeared as abstracts (Dobrunz et al., 1993, 1994).

MATERIALS AND METHODS

Experiments were performed on right ventricular trabeculae from male LBNF1 rats each weighing 150–200 g (Harlan, Indianapolis, IN). Anesthesia was induced using diethyl ether (J. T. Baker Chemical Co., Phillipsburg, NJ), and the heart was rapidly excised. Retrograde perfusion with a high K^+-modified Krebs-Henseleit solution (described below) via the aortic stump was used to flush blood from the heart and to arrest the heart during dissection. A suitable trabecula was removed from the right ventricle along with a small piece of the ventricular wall at the base and the section of the atrioventricular valve where the trabecula inserted. The muscle was mounted in the experimental chamber (solution described below) and stimulated at 0.5 Hz for 1 h to allow equilibration. During that time the muscle was gradually stretched to L_{max}, the length that maximized developed twitch tension without causing an extensive increase in passive tension. Although sarcomere length was not measured in these experiments, L_{max} corresponded to a measured sarcomere length of 2.2–2.3 μm in a parallel set of experiments. Importantly, internal shortening is minimal (3–7%) in this preparation over this range of sarcomere lengths (ter Keurs et al., 1980), thereby facilitating straightforward interpretation of our results despite the lack of dynamic sarcomere length control. Muscles were 2.11 ± 0.63 mm in length at L_{max} (n = 12, mean ± SD throughout), 193 ± 53 μm wide, and 84 ± 28 μm thick, with an average maximal tension (F_{max}) of 118.2 ± 26.5 mN/mm^2, measured as described below.

The dissection and muscle chamber perfusion solutions were a modified Krebs-Henseleit solution consisting of 119.5 mM NaCl, 5.0 mM KCl, 1.2 mM $MgSO_4$, 19 mM $NaHCO_3$, 2.0 mM NaH_2PO_4, and 10 mM glucose. (All chemicals were obtained from Sigma Chemical Co., St. Louis, MO, except as listed below.) The dissection solution contained an additional 10 mM KCl; the $CaCl_2$ concentration was 0.5 mM. The muscle chamber perfusion solution contained 0.5 mM $CaCl_2$ during the initial muscle equilibration; the $CaCl_2$ concentration was altered throughout the experiment, as described below. Solutions were bubbled with 95% O_2/5% CO_2 (Puritan-Bennett, Linthicum Heights, MD), and pH was adjusted to 7.4. Temperature was maintained at 22°C.

Fig. 1 shows a diagram of the experimental setup. The piece of ventricular wall at the base of the trabecula was placed in a cradle (de Tombe and ter Keurs, 1990) attached to a force transducer (BG-10, Kulite Semiconductor Products, Inc., Leonia, NJ). The piece of valve at the other end of the trabecula was impaled on a pin attached to a fixed support (provided by the arm of a Model 300B ergometer, Cambridge Technology, Cambridge, MA). The muscle was field-stimulated via two parallel platinum wire electrodes with supramaximal, monopolar pulses 12 ms in duration. During the initial equilibration and the equilibration after Fura-2 loading, the muscle was stimulated at 0.5 Hz; during the experimental protocol, the stimulus rate was reduced to 0.2 Hz to allow full relaxation of the slowed twitches between beats. The output of the Kulite transducer was filtered at 100 Hz (Model 902, 8-pole 3-dB Bessel filter, Frequency Devices, Haverhill, MA), acquired digitally at a sampling rate of 1 kHz (DT2821, Data Translation, Inc., Marlboro, MA) and stored by computer for analysis.

Ultraviolet light to excite the Fura-2 was supplied by a 75-W xenon arc lamp (Oriel Corporation, Stratford, CT), which was band-pass-filtered at 340 nm, 358 nm, or 380 nm using band-pass filters (10-nm bandwidth, Omega Optical, Brattleboro, VT) contained in a computer-controlled filter wheel (model 77374, Oriel Corporation). Light was projected directly onto a dichroic mirror (400DPLC, Nikon, Tokyo, Japan) and reflected through the 10× objective of an inverted microscope (CK-2, Olympus Optical Co., Ltd., Tokyo, Japan) to illuminate the muscle. Emitted light was recorded at 510 nM (40-nM bandwidth band-pass filter, Omega Optical) using a photomultiplier tube (R2693, Hamamatsu Photonics K.K., Bridgeport, NJ) attached to the camera port of the inverted microscope. The resulting signal was filtered at 100 Hz (Model 902, 8-pole 3-dB Bessel filter, Frequency Devices) and sampled by an analog/digital board (DT2821, Data Translation) at 300 Hz to 1 kHz.

Fura-2 salt (Molecular Probes, Inc., Eugene, OR) was loaded into the trabeculae via iontophoretic injection, as described by Backx and ter Keurs (1993). Briefly, a micropipette containing 1 mM Fura-2 salt in 150 mM KCl was used to impale the trabecula at one to three sites. The micropipette holder was attached to the probe of a Microprobe system M-707A (World Precision Instruments, New Haven, CT). Negative current (4–6 nA) was passed into the (unstimulated) muscle, which caused Fura-2 to enter the cell and diffuse throughout the preparation via the gap junctions. After Fura-2 injection, the muscle was stimulated at 0.5 Hz and allowed to equilibrate for 1 h, after which time the dye seemed to be uniformly distributed.

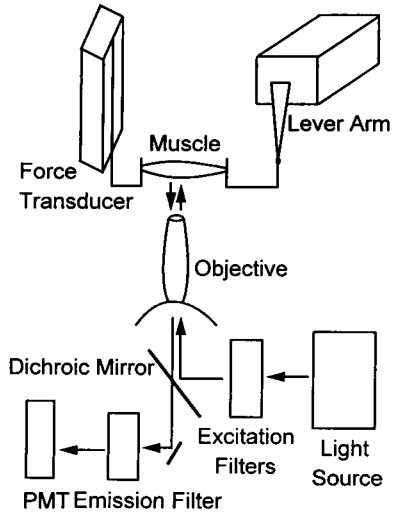

FIGURE 1 Block diagram of experimental setup.

Autofluorescence was always measured before Fura-2 loading and often measured again at the end by washing with a Ca^{2+}-free Krebs-Henseleit solution containing 10–50 μM ionomycin (Calbiochem, La Jolla, CA) and 0.5 mM Mn^{2+} to quench the Fura-2 fluorescence. We saw no detectable difference in the autofluorescence measured at the end of the experiment as compared with that measured before loading the Fura-2. The ratio of the fluorescent signal elicited by illumination at 340 nM to that elicited by illumination at 380 nM (after subtracting autofluorescence from each signal) is independent of the dye concentration (Grynkiewicz et al., 1985); the ratio is converted to $[Ca^{2+}]_i$ using the equation (Grynkiewicz et al., 1985):

$$[Ca^{2+}]_i = K'_d \frac{R - R_{min}}{R_{max} - R} \quad (1)$$

where K'_d is the apparent dissociation constant, R is the ratio of 340 nM to 380 nM fluorescence, R_{min} is the minimum value of R obtained at zero $[Ca^{2+}]_i$, and R_{max} is the maximum value of R obtained at saturating levels of $[Ca^{2+}]_i$ (5 mM). These calibration values were obtained as described in Backx and ter Keurs (1993), resulting in R_{max} = 7.72, R_{min} = 0.25, K'_d = 4.64 μM.

The protocols are summarized as follows. In four preparations, twitch force and $[Ca^{2+}]_i$ were measured before addition of CPA and ryanodine at 3–4 $[Ca^{2+}]_o$ in the range 0.5–1.5 mM. In 12 trabeculae, 50 μM CPA (Seidler et al., 1989), and 1 μM ryanodine (Sutko and Willerson, 1980; Sutko et al., 1985) were added to block the uptake and phasic release of Ca^{2+} from the SR. This greatly slowed twitch time course and also prevented spontaneous contractions normally caused by calcium overload at high $[Ca^{2+}]_o$. After slowing of contraction time course, control twitch force and $[Ca^{2+}]_i$ transients were measured at four to six levels of $[Ca^{2+}]_o$ ranging from 0.5–6.0 mM. Afterward, maximum Ca^{2+}-activated force (F_{max}) was measured during tetanus induced by several seconds of 8–10-Hz stimulation with 5-ms pulses at 6.0 mM $[Ca^{2+}]_o$. The perfusion solution was then replaced with an identical solution (Krebs-Henseleit, 50 μM CPA, 1 μM ryanodine) at low calcium (0.5–1.5 mM $[Ca^{2+}]_o$), and the effect of either 1 μM isoproterenol (n = 6) or 2 μM EMD 53998 (n = 4) was tested. EMD 53998 [5-(1-(3, 4-dimethoxybenzoyl)-1,2,3,4-tetrahydro-6-quinolyl)-6-methyl-3,6-dihydro-2*H*-1,3,4-thiadiazin-2–1] was kindly provided by Dr. M. Klockow, E. Merck Pharmaceuticals, Darmstadt, Germany. The series of measurements of twitch force and $[Ca^{2+}]_i$ at 0.5–6.0 mM $[Ca^{2+}]_o$ was then repeated, and F_{max} was measured again. Plots of twitch force versus $[Ca^{2+}]_i$ were superimposed for different $[Ca^{2+}]_o$ for both control and isoproterenol or EMD conditions. As explained below, the regions of these curves that overlap during the relaxation phase of the twitch at different $[Ca^{2+}]_o$ are interpreted as being in steady state and were fitted with the Hill equation:

$$F = \frac{F_{max}[Ca^{2+}]_i^{n_H}}{K_{1/2}^{n_H} + [Ca^{2+}]_i^{n_H}} \quad (2)$$

Hill functions were used only for purposes of approximate quantitation to facilitate numerical comparison of curves and to enable statistical analysis. We in no way imply that the Hill function provides an exact fit to the data; in fact, there are small quantitative differences of the data from the idealized Hill relation (see Fig. 4 *B*), but these minor deviations are secondary to the major modulatory events described here. Numerical fits were performed by holding fixed the experimentally determined F_{max} (described above) and by varying the parameters $K_{1/2}$ (the $[Ca^{2+}]_i$ that corresponds to one-half the F_{max}) and n_H (the Hill coefficient, an indication of steepness of the curve). All results are presented as mean ± SD. Student's two-tailed paired t-test was used to test for statistical differences between control and isoproterenol or EMD for F_{max}, $K_{1/2}$, and n_H, with $p < 0.02$ considered significant.

EXPERIMENTAL RESULTS

Fig. 2 *A* shows twitch force and $[Ca^{2+}]_i$ transients before and after addition of 50 μM CPA and 1 μM ryanodine. Note that the amplitudes of both force and $[Ca^{2+}]_i$ transients are significantly reduced by CPA and ryanodine. Fig. 2 *B* shows the $[Ca^{2+}]_i$ transients from control and with CPA and ryanodine (from *A*) normalized to the same peak amplitude. This illustrates the prolonged time course with CPA and ryanodine. Likewise, Fig. 2 *C* shows normalized force transients from control and with CPA and ryanodine (from *A*), revealing that the force time course is also slowed by CPA and ryanodine.

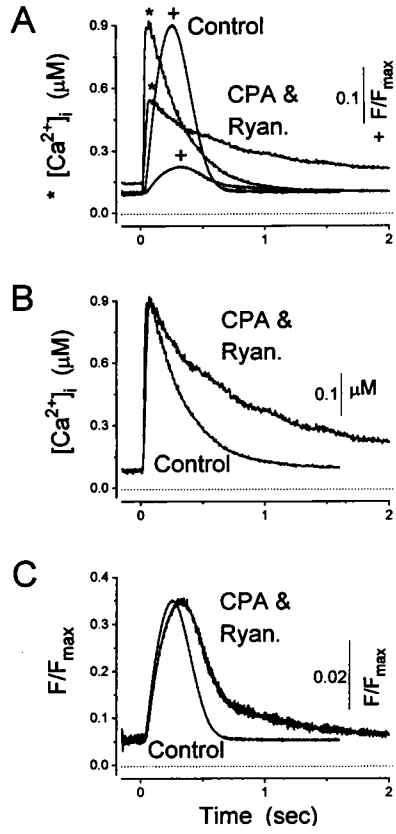

FIGURE 2 Force (+) and $[Ca^{2+}]_i$ (*) versus time in an isolated rat trabecula iontophoretically loaded with Fura-2 salt. (*A*) Force and $[Ca^{2+}]_i$, 0.5 mM $[Ca^{2+}]_o$, before (Control) and after addition of 50 μM CPA and 1 μM ryanodine (CPA & Ryan.). Forces are normalized to F_{max}, measured as described in the Methods section, except where noted. (*B*) $[Ca^{2+}]_i$ transients, control and with CPA and ryanodine (from *A*), normalized to same peak amplitude to illustrate prolonged time course with CPA and ryanodine. Scale bar indicated 0.1 μM $[Ca^{2+}]_i$ for trace with CPA and ryanodine. (*C*) Force transients, control, and with CPA and ryanodine (from *A*), normalized to same peak amplitude to illustrate prolonged time course with CPA and ryanodine. Scale bar indicates 0.02 F/F_{max} for trace with CPA and ryanodine. All experiments at 22°C. All panels from muscle 931201.

Addition of CPA and ryanodine also enables tetanization, which was used at high $[Ca^{2+}]_o$ to measure F_{max} (Yue et al., 1986). F_{max} was measured in each muscle to allow normalization and to facilitate comparison between preparations. Fig. 3 *A* shows a representative tetanus used to measure F_{max} with force displayed in mN/mm^2; all other figures display normalized forces (F/F_{max}). Notice in Fig. 3 *A* that $[Ca^{2+}]_i$ continues to increase even though force is constant or slightly falling. We found that addition of Bay K 8644

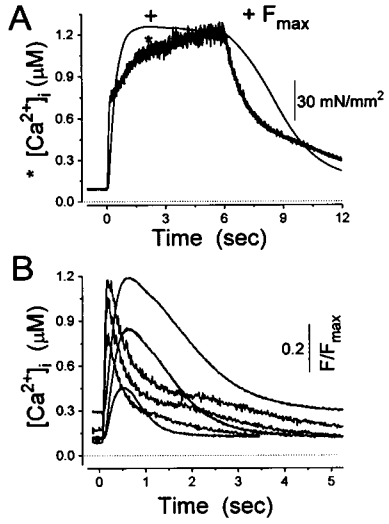

FIGURE 3 (*A*) Force and $[Ca^{2+}]_i$ versus time during a typical 10-Hz tetanus used to measure F_{max}, 6.0 mM $[Ca^{2+}]_o$ with CPA and ryanodine. Muscle 940510. (*B*) Typical $[Ca^{2+}]_i$ and force transients at 3.0, 4.5, and 6.0 mM $[Ca^{2+}]_o$ with CPA and ryanodine. Muscle 930812.

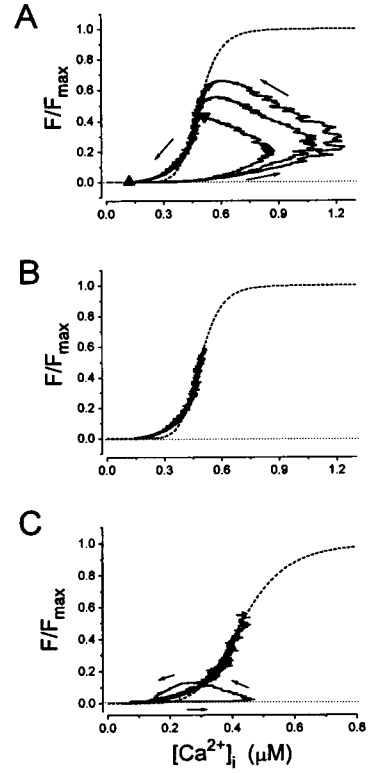

FIGURE 4 Force-$[Ca^{2+}]_i$ relationship derived from twitches slowed with CPA and ryanodine. (*A*) Force versus $[Ca^{2+}]_i$ loops from entire twitch at 3.0, 4.5, and 6.0 mM $[Ca^{2+}]_o$. Symbols are used on smallest trajectory to indicate time points: ◆ occurs 0.3 s after stimulation, ▼ occurs 0.63 s after stimulation, and ▲ occurs 5 s after stimulation. Arrows indicate direction traversed during twitch. (*B*) Steady-state force-$[Ca^{2+}]_i$ relationship consists of regions from *A* where trajectories overlap. Dashed curve is best fit of Hill equation (see text) to data, with $K_{1/2}$ = 0.48 μM and n_H = 6.9. Muscle 940503 for panels *A* and *B*. (*C*) Entire force-$[Ca^{2+}]_i$ loop measured in a different muscle before addition of CPA and ryanodine, and steady-state force-$[Ca^{2+}]_i$ relationship. Dashed curve indicates best fit of Hill equation (see text) to steady-state data, with $K_{1/2}$ = 0.43 μM and n_H = 6.0. Arrows indicate direction traversed during twitch. Muscle 931113.

(Miles Inc., West Haven, CT), a Ca^{2+} channel agonist (Brown et al., 1984), caused a further increase in $[Ca^{2+}]_i$ with no change in force, confirming that F_{max} was indeed measured (n = 2). Bay K 8644 has been shown not to alter myofilament Ca^{2+} sensitivity or F_{max} (Thomas et al., 1985).

At higher $[Ca^{2+}]_o$ the prolongation of time course is quite dramatic. Fig. 3 *B* shows twitches obtained at three different $[Ca^{2+}]_o$ in the presence of CPA and ryanodine. The $[Ca^{2+}]_i$ transients (noisy traces) and the force transients (smoother traces) both demonstrate progressive slowing of the late phase of relaxation (notice the different time scales between Figs. 2 *B* and 3 *B*). Without the rapid removal of Ca^{2+} from the cytosol by the SR, $[Ca^{2+}]_i$ decline during twitch relaxation is most likely limited by the much slower rate of Ca^{2+} efflux across the sarcolemma. $[Ca^{2+}]_i$ is thus changing slowly enough to allow force and $[Ca^{2+}]_i$ to reach steady state during relaxation, such that force at any one time depends only on the instantaneous $[Ca^{2+}]_i$ and not on the history of contraction.

This is best illustrated by relating force and $[Ca^{2+}]_i$ by a plot of twitch force versus the $[Ca^{2+}]_i$ measured at that time. Three such loops obtained at three different $[Ca^{2+}]_o$ are superimposed in Fig. 4 *A*. The arrows indicate the direction the loop is traversed during a twitch. Note that during the later portion of the curves (which correspond to relaxation and force decline), the curves fall along an apparently unique trajectory, independent of contraction history. Because $[Ca^{2+}]_i$ and force can be uniquely related only at steady state, we tentatively interpret the overlapping regions of the curves in Fig. 4 *A* (redrawn in Fig. 4 *B*) as the steady-state force-$[Ca^{2+}]_i$ relationship. By contrast, force-$[Ca^{2+}]_i$ plots measured without CPA and ryanodine plots do not follow a common trajectory, as the history of contraction varies. In fact, the force-$[Ca^{2+}]_i$ loops are almost entirely distinct from the measured steady-state relationship. Fig. 4 *C* shows data from a different muscle in which one such loop is superimposed upon its corresponding steady-state relationship.

Because our force-$[Ca^{2+}]_i$ relationships are not determined in a traditional manner (in which the occupancy of the various molecular states is not changing), it is worth considering how a virtual steady state arises despite the decrease in force and $[Ca^{2+}]_i$. The important feature is that $[Ca^{2+}]_i$ is probably changing slowly enough to become the rate-limiting step in force decline. Therefore, the intermediate steps linking $[Ca^{2+}]_i$ to force can reach steady state relative to the rate of Ca^{2+} removal. Such a scenario is plausible, given that the time constant for force decay in response to a step decrease in $[Ca^{2+}]_i$ is approximately 150 ms in cardiac muscle (Simnett et al., 1993), and force declines with a time constant of >1 s in our slowed twitches. Therefore it is quite likely that Ca^{2+} removal (not thin-filament deactivation or cross-bridge kinetics) is the rate-limiting factor. Plausibility aside, the key experimental

support for our contention that our force-$[Ca^{2+}]_i$ relationships reflect steady-state behavior resides in the uniqueness of force-$[Ca^{2+}]_i$ trajectories during relaxations. It might be questioned whether twitches of the sort in Fig. 4 *A* are sufficiently varied to prove that the fixed trajectory is truly independent of contraction history.

To bolster the suggestion that the overlapping force-$[Ca^{2+}]_i$ plots obtained during slow relaxation represent a unique trajectory, we tested whether the relationship is altered by two very different types of perturbations. Fig. 5, *A* and *B*, shows force and $[Ca^{2+}]_i$ versus time for a twitch and 2-s tetanus. Fig. 5 *C* demonstrates that the relaxation phases of twitch and tetanic force-$[Ca^{2+}]_i$ loops are identical. Furthermore, Fig. 5 *D* demonstrates that force-$[Ca^{2+}]_i$ relations from relaxing twitches agree entirely with discrete measurements derived from plateaus of force and $[Ca^{2+}]_i$ (*solid circles*) during 1–2 s of tetanic stimulation at different $[Ca^{2+}]_o$. The latter estimates of the steady-state force-$[Ca^{2+}]_i$ relationship emerge from the traditional analysis of tetanic data (Yue et al., 1986; Gao et al., 1994). An even more stringent test is illustrated in Fig. 6, where muscle length is transiently decreased by 5% during relaxation of a slowed twitch. Fig. 6, *A* and *B*, shows superimposed $[Ca^{2+}]_i$ and force waveforms for twitches with and without a length perturbation. When replotted as force-$[Ca^{2+}]_i$ trajectories (Fig. 6 *C*), it is clear that the length change induces a temporary displacement from the steady-state relationship (deviation marked by *solid arrow*), as might be expected from the interrelation between muscle length and myofilament $[Ca^{2+}]_i$ sensitivity in skinned muscle (Fabiato and Fabiato, 1978a). The important new result comes with restoration of the muscle to its initial length, whereupon the trajectory returns to

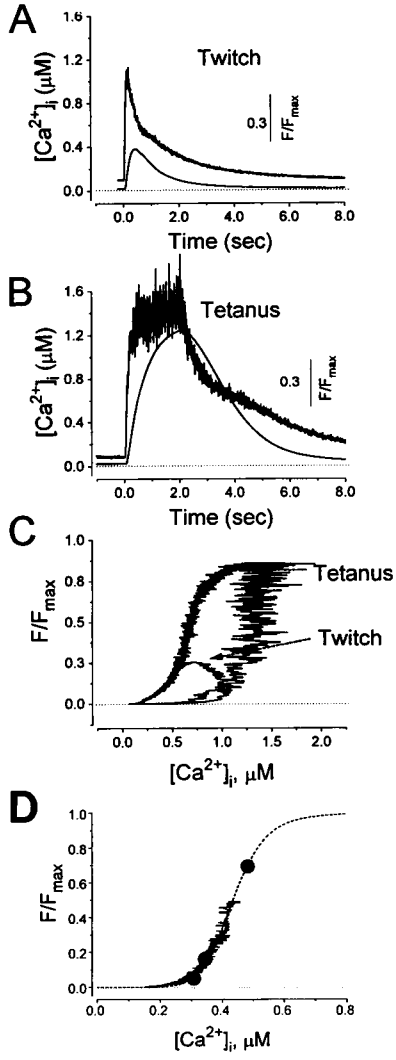

FIGURE 5 Additional perturbation to test uniqueness of steady-state force-$[Ca^{2+}]_i$ curves derived as in Fig. 3. (*B*) $[Ca^{2+}]_i$ and force versus time during a short tetanus (2 s of 10-Hz stimulus, 50-ms pulse duration, at 0.5 mM $[Ca^{2+}]_o$); (*C*) relaxation phase of force-$[Ca^{2+}]_i$ loop from tetanus in *B* directly coincides with force-$[Ca^{2+}]_i$ trajectories from twitch in *A*. Panels *A-C* from muscle 940607. (*D*) Force-$[Ca^{2+}]_i$ trajectories of relaxing twitches coincide with discrete force-$[Ca^{2+}]_i$ measurements (*solid circles*) during 1–2 s of 10-Hz tetanic stimulation at three different $[Ca^{2+}]_o$. Dashed curve is Hill fit to twitch trajectories, subject to experimentally determined maximal force, as in Fig. 3*A*. Muscle 940928.

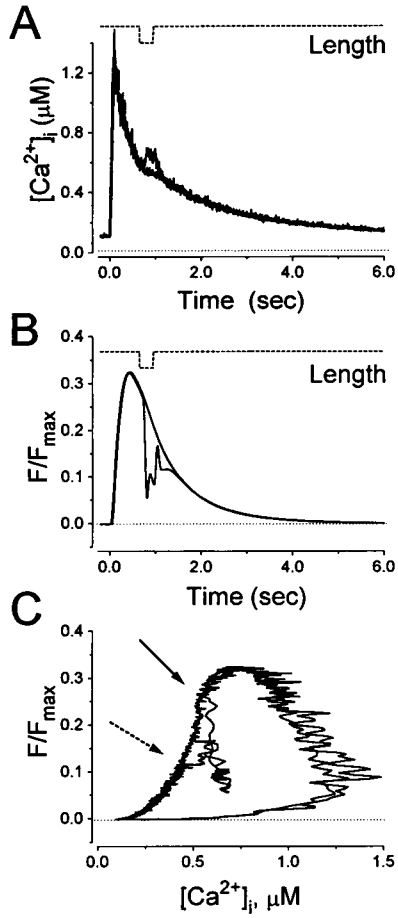

FIGURE 6 Perturbation in muscle length to test uniqueness of steady-state force-$[Ca^{2+}]_i$ curves derived as in Fig. 3. (*A*) $[Ca^{2+}]_i$ and (*B*) force versus time during slowed twitch where length perturbation (specified by *dashed line*) was applied. Length was decreased from 100% L_{max} to 95% L_{max} for a 300-msec pulse applied approximately 400 msec after the stimulus; (*C*) trajectory deviates from steady-state curve during length perturbation (start of deviation marked with *solid arrow*) but returns to steady-state relationship after muscle is returned to original length (marked with *dashed arrow*). All panels from muscle 940607.

the measured steady-state relationship (*dashed arrow* marks return to steady-state relationship within 300 ms of resetting length to 100% L_{max}). Taken together, the results (Fig. 4 *A*, Fig. 5, *C* and *D*, and Fig. 6 *C*) provide unequivocal evidence that our force-$[Ca^{2+}]_i$ relationships are unique and therefore reflect genuine steady-state properties.

Having validated our method for obtaining in vivo steady-state force-$[Ca^{2+}]_i$ relationships, we investigated the effect of β-adrenergic stimulation. Fig. 7 *A* shows the effects of 1 μM isoproterenol on force and $[Ca^{2+}]_i$ time course in this SR-modified preparation. Note that peak $[Ca^{2+}]_i$ amplitude and $[Ca^{2+}]_i$ transient duration are both augmented by isoproterenol. Because SR Ca^{2+} release does not contribute to $[Ca^{2+}]_i$ here, the increased $[Ca^{2+}]_i$ is likely caused by β-adrenergic enhancement of Ca^{2+} influx through sarcolemmal channels (Bean et al., 1984). Fig. 7 *B* shows the steady-state force-$[Ca^{2+}]_i$ relationships obtained from this muscle during control and isoproterenol-treated twitches. They demonstrate that β-adrenergic stimulation produces a dramatic rightward shift and a decrease in slope of the relationship, with no change in F_{max}. The dashed lines show fits of the Hill equations to this data, normalized to F_{max} from control.

Both effects of isoproterenol were consistently observed, as shown in Table 1 ($n = 6$). Isoproterenol increases $K_{1/2}$ to 215 $\pm$ 71% ($p < 0.01$) and decreases the Hill coefficient to 73 $\pm$ 12% ($p < 0.01$) of the control values, with no change in F_{max} (99 $\pm$ 2% of control). The overall magnitude of the modulation is illustrated graphically in Fig. 8, which shows curves generated by the Hill equation using the average parameters for the six preparations. A similar effect was produced by addition of 1 mM 8-bromo-cAMP (L.E. Dobrunz and D.T. Yue, unpublished data), a membrane-permeable analog of cAMP. cAMP, the second messenger involved in β-adrenergic stimulation (Tsien, 1977), leads to phosphorylation of intracellular sites in cardiac muscle, including troponin I (TnI) (Holroyde et al., 1979; Ray and England, 1976).

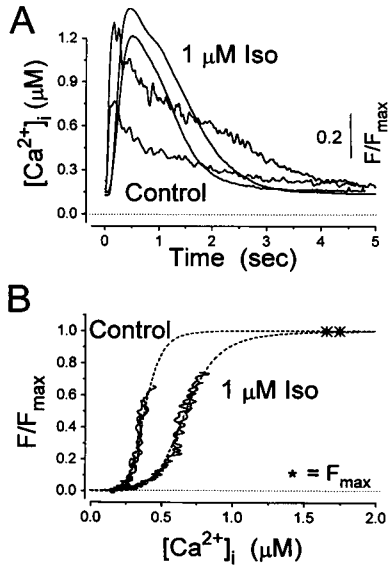

FIGURE 7 Effects of isoproterenol. (*A*) Force (normalized to F_{max}) and $[Ca^{2+}]_i$ versus before and after adding 1 μM isoproterenol; (*B*) steady-state force-$[Ca^{2+}]_i$ relationship, before and after addition of 1 μM isoproterenol. Dashed curves are best fits of Hill equation (see text) to data, with $K_{1/2} = 0.38$ μM and $n_H = 6.5$ for the control and $K_{1/2} = 0.63$ μM and $n_H = 5.8$ with isoproterenol. * indicates experimentally measured F_{max} from tetani as in Fig. 5 *B*. All panels from muscle 930702.

We also investigated the effect of 2 μM EMD on the steady-state force-$[Ca^{2+}]_i$ relationship. Typical force and $[Ca^{2+}]_i$ transients are shown in Fig. 9 *A* from twitches in control and after addition of 2 μM EMD (EMD traces indicated by *arrows*). Notice that EMD dramatically increases the amplitude of twitch force and significantly prolongs the time course. However, the $[Ca^{2+}]_i$ transient is affected only minimally by EMD; there is no large increase in peak $[Ca^{2+}]_i$, as would be expected if the inotropic effect was caused by increased $[Ca^{2+}]_i$.

Fig. 9 *B* displays steady-state force-$[Ca^{2+}]_i$ relationships obtained during control and EMD exposure. EMD causes a clear leftward shift of this relationship, without an obvious change in steepness. The dashed curves in Fig. 9 *B* show fits of the Hill equation to this data, normalized to F_{max} measured in control. Notice that EMD also increases F_{max}.

EMD consistently produced a leftward shift of the force-$[Ca^{2+}]_i$ relationship. Table 1 lists average $K_{1/2}$ and n_H from four experiments, indicating that $K_{1/2}$ was decreased to 71 $\pm$ 12% of the control ($p < 0.02$). However, there was no significant change in the Hill coefficient (101 $\pm$ 20% of control). The F_{max} that the muscle was able to generate was increased to 107.1 $\pm$ 4.6% by 2 μM EMD. Although this effect was relatively small in magnitude, it was consistent and statistically significant ($p < 0.005$). The overall effects of EMD are illustrated graphically in Fig. 10, which shows the curves generated by the Hill equation and the average of the Hill parameters for the four preparations.

QUANTITATIVE MODEL OF COOPERATIVE, THIN-FILAMENT ACTIVATION

To articulate mechanisms involved in modulating myofilament calcium sensitivity, this section develops a simple model of thin-filament activation that explicitly incorporates the major proposed sources of cooperative interactions in force development. Fig. 11 *A* diagrams the dominant states of the fundamental regulatory unit (RU), as well as allowable interstate transitions (*solid arrows*). State U corresponds to an RU in which Ca^{2+} is not bound

TABLE 1 Summary of Hill equation fits to force-$[Ca^{2+}]_i$ relationships with isoproterenol and EMD

	$K_{1/2}$ (μM)	n_H
Control	0.389 $\pm$ 0.069	5.39 $\pm$ 1.09
Iso	0.820 $\pm$ 0.230*	4.05 $\pm$ 1.37*
Control	0.421 $\pm$ 0.019	5.98 $\pm$ 0.59
EMD	0.302 $\pm$ 0.061‡	6.02 $\pm$ 1.07

*Statistically significant, $p < 0.01$.
‡Statistically significant, $p < 0.02$.

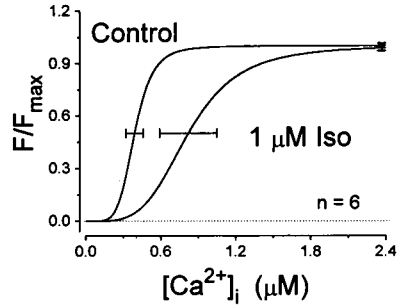

FIGURE 8 Summary of effects of 1 μM isoproterenol on force-$[Ca^{2+}]_i$ relationship showing Hill curves generated from the average of parameters from Hill equation fits to individual data sets, mean ± SD, $n = 6$.

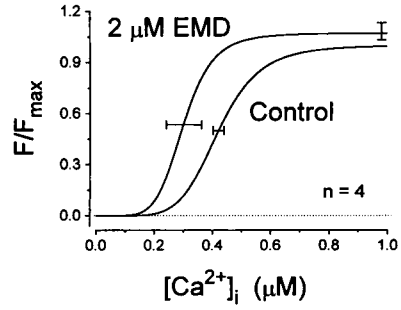

FIGURE 10 Summary of effects of 2 μM EMD on force-$[Ca^{2+}]_i$ relationship showing Hill curves generated from the average of parameters from Hill equation fits to individual data sets, mean ± SD, $n = 4$.

to troponin C (TnC), and in which Tm (tropomyosin) is positioned to render actin inactive in relation to strong myosin attachment. Ca^{2+} can bind to TnC, forming state B, which is still inactive. However, the presence of bound Ca^{2+} biases Tm to shift conformation so as to render actin reactive to strong myosin binding, as diagrammed for state B*. In the reactive configuration, the entire RU is assumed to be receptive to strong cross-bridge attachment. For simplicity, B* in this formulation represents a compound state in which substates, with (B^*_M) and without (B^*_O) strong myosin attachment, are considered to be in rapid equilibrium according to apparent strong-binding cross-bridge (de)attachment rates f and g (Huxley, 1957; but see Brenner, 1988). Hence, $B^*_M/B^*_O = f/g$. Likewise, U* represents another compound, reactive state in which Tm permits strong myosin binding, but no Ca^{2+} is bound to TnC in this conformation. U^*_M and U^*_O are the actual substates of U* that are distinguished by the presence or absence of strong myosin attachment, respectively. $U^*_M/U^*_O = f/g$ by the rapid equilibrium assumption. Force is therefore proportional to the total probability of reactive units multiplied by the duty cycle for strong myosin attachment ($(U^* + B^*) * f/(f + g)$). We only consider strong, binding cross-bridges here because the experiments measure force.

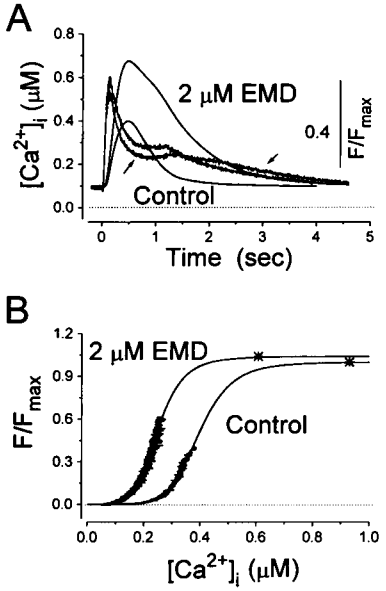

FIGURE 9 Effects of EMD. (*A*) Force (normalized to F_{max}) and $[Ca^{2+}]_i$ versus before and after adding 2 μM EMD; $[Ca^{2+}]_i$ curve with EMD crosses the control and is indicated by arrows. Muscle 930818. (*B*) Steady-state force-$[Ca^{2+}]_i$ relationship, before and after addition of 2 μM EMD. Dashed curves are best fits of Hill equation (see text) to data, with $K_{1/2} = 0.38$ μM and $n_H = 6.5$ for the control and $K_{1/2} = 0.25$ and $n_H = 6.5$ with EMD. Muscle 940601. The unusual biphasic shape of the $[Ca^{2+}]_i$ transient during relaxation in panel *A* (both control and with EMD) is sometimes seen in muscles with CPA and ryanodine, especially at higher $[Ca^{2+}]_o$. Although the exact cause is unknown, we believe it reflects the different time courses of Ca^{2+} binding to TnC (early, more rapid phase of $[Ca^{2+}]_i$ decline) and Ca^{2+} extrusion across the sarcolemma (late, slow phase of $[Ca^{2+}]_i$ decline).

We were interested in obtaining quantitative solutions for the steady-state relationship between occupancy of the various states and $[Ca^{2+}]_i$, a daunting challenge when one considers a large, linear network of RUs that can interact according to the cooperative mechanisms described below (Fig. 11 *C*). For simplicity of solution, we make the approximation that microscopic reversibility is preserved across each of the four main transitions for each unit, denoted by solid arrows in Fig. 11 *B*. This approximation implies that the steady-state probabilities of occupying various states are completely specified by the equilibrium constants shown in Fig. 11 *B*, in which the constants are formulated by considering states at the end of arrows as products. Specifically, the following ratios of steady-state probabilities are specified as:

$$U^*/U = K_a * (1 + f/g) * \gamma^p = K'_a \quad (3a)$$

$$B/U = K_c * [Ca^{2+}]_i \quad (3b)$$

$$B^*/B = K_b * (1 + f/g) * \gamma^p = K'_b \quad (3c)$$

and

$$B^*/U^* = K_c * [Ca^{2+}]_i * K_b/K_a \quad (3d)$$

where K_a and K_b are affinity constants for transitions from inactive to reactive forms, γ and p are cooperativity factors defined below, and K_c is the affinity constant for Ca^{2+} binding to TnC. The apparent affinity constants K'_a and K'_b constrain the

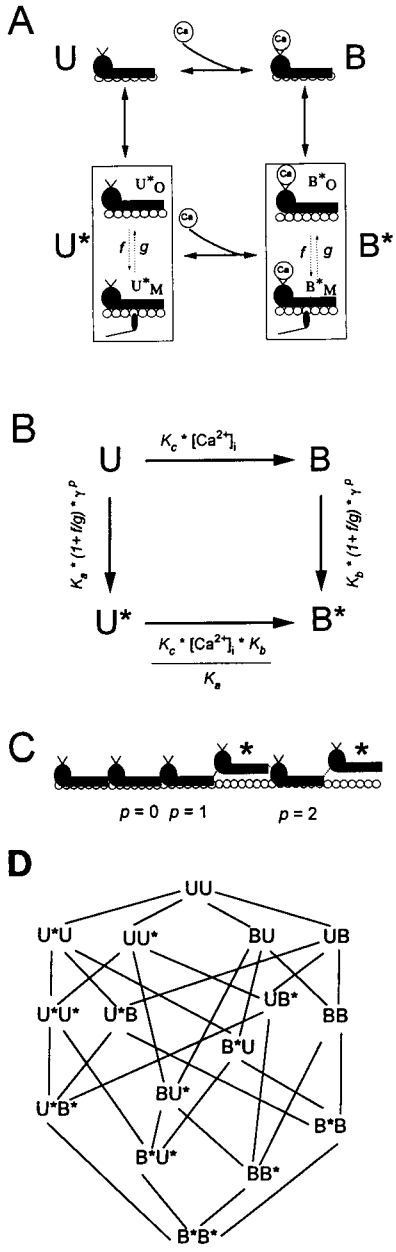

FIGURE 11 Model of steady-state cooperative force development. (*A*) Pictorial representation of model states and allowable transitions; (*B*) equilibrium constants for allowable transitions; (*C*) example of model with 6 consecutive RUs to demonstrate meaning of p, the number of reactive nearest neighbors (marked by *) of a given unit. Shown are possible cooperative interactions when $p = 0$, $p = 1$, or $p = 2$. (*D*) State diagram showing possible transitions for 2-unit model.

steady-state probability ratio between inactive and reactive forms (U/U* and B/B*, respectively). The expressions for these two terms can be derived from the definitions $U_O^*/U = K_a \gamma^p$ and $U^*/U = (U_O^* + U_M^*)/U = (U_O^*/U)(1 + U_M^*/U_O^*)$. Substituting the first definition into the rightmost expression for the second definition yields $U^*/U = K_a \gamma^p (1 + U_M^*/U_O^*)$. Because we assume that U_M^* and U_O^* are in rapid equilibrium, the parenthetical expression is $(1 + f/g)$, yielding Eq. 3a. A similar argument can be used to derive the expression for K_b'. Eq. 3d is required to conform with the requirements of microscopic reversibility across each of the four main transitions, as follows. Microscopic reversibility requires that

$$(U_O^*/U)(B_O^*/U_O^*)(B/B_O^*)(U/B) = 1$$

Hence, from Eq. 3a–c,

$$B_O^*/U_O^* = K_c [Ca^{2+}]_i K_b/K_a.$$

We are actually interested in an expression for B*/U*, which is related to B_O^*/U_O^* by $B^*/U^* = (B_O^*/U_O^*)[(1 + B_M^*/B_O^*)/(1 + U_M^*/U_O^*)]$. From the rapid equilibrium assumption, $B_M^*/B_O^* = U_M^*/U_O^* = f/g$, so that the parenthetical terms cancel out. Hence, $B^*/U^* = B_O^*/U_O^*$, such that we have Eq. 3d. Eq. 3 forms the general foundation for solving the model.

Cooperative interactions present a special challenge. Their effects are explicitly manifest as variations in K_a' and K_b' as a function of the state of adjacent RUs and myosin attachment. First, consider thin-filament interaction between adjacent Tm molecules. If both adjacent RUs are inactive ($p = 0$ case in Fig. 11 *C*), then the steady-state probability ratio between reactive and inactive states on the specified RU are given by $U/U^* = K_a' = K_a^*(1 + f/g)$ and $B/B^* = K_b' = K_b^*(1 + f/g)$. If one adjacent RU is reactive ($p = 1$ case in Fig. 11 *C*), then tethering (Leavis and Gergeley, 1984) between adjacent Tm molecules should stabilize reactive versus inactive conformations of the specified unit by an interaction energy G_i (<0), such that the apparent affinity constants K_a' and K_b' should be increased by a factor $\gamma^1 = \exp(-G_i/RT) > 1$. If both adjacent RUs are reactive ($p = 2$ case in Fig. 11*C*), then the net stabilization of reactive versus inactive conformations corresponds to an interaction energy of $2G_i$, such that apparent affinity constants K_a' and K_b' should now be increased over the $p = 0$ case by a factor $\gamma^2 = \exp(-2G_i/RT) > 1$. These interactions gives rise to the p terms in Eq. 3a and c, where p enumerates adjacent neighbors (0, 1, or 2) in the reactive configuration (U* or B*). A second type of interaction arises from the proposed stabilization of reactive versus inactive forms by strong binding of myosin itself (Bremel and Weber, 1972). Accordingly, the model does not permit direct transitions from the myosin-attached substates, U_M^* and B_M^*, to either U or B. Although an RU is in U* or B*, transitions to U or B may only transpire during that fraction of time spent in the myosin-unattached substate ($g/(f + g)$).

With these properties in hand, we formulate a state diagram for an entire linear network of RUs. Fig. 11 *D* shows an example for a system with two adjacent RUs on the thin filament. States between which transitions are allowed are connected with solid lines and are associated with equilibrium constants that are completely specified in Eq. 3a–d. The steady-state behavior of such a network can therefore be derived from the equilibrium solution to the diagram. In practice, model systems with ≈9 RUs were required before parameter estimates became independent of the number of units in the model network, as might be expected in vivo given an estimate of ≈26 RUs per thin filament (Brandt et

al., 1987). The requisite network size seems reasonable, given the experimentally determined force-$[Ca^{2+}]_i$ relations with Hill coefficients of 4–6. Therefore, results from 9-unit networks were used in the analysis in the Quantitative Model Results section to follow.

The steady-state solution to a linear network of RUs was obtained by a simple numerical method. For a system of L sequential RUs, each with four possible conformations (U, B, U*, and B*), the number of system states in the model is 4^L. The 2-unit model therefore has 16 states; the 9-unit model that we actually used has 262,144 states. Analytical solution of the network model proved too cumbersome. We developed instead a string-handling computer program that tallies all possible states of the regulatory network, as well as all possible transitions.

Taking advantage of this list of states and transitions, another portion of the program solves for the steady-state probabilities of every state as follows. The equilibrium assumption simplifies this task because the equilibrium constant relating any two states is now the product of equilibrium constants of transitions along any path connecting the two states. The first task of the program is to formulate the steady-state probabilities of every state in terms of the probability of occupying the state containing all Us. For example, in the simple 2-unit model in Fig. 11 *D*, the procedure involves generating the following type of equations for all states:

$$BU = K_c * [Ca^{2+}]_i * UU \quad (4a)$$

$$BB = K_c * [Ca^{2+}]_i * BU \quad (4b)$$

$$= (K_c * [Ca^{2+}]_i)^2 * UU \quad (4c)$$

where UU, BU, and BB indicate the steady-state probabilities of the model occupying each of those states. The full spectrum of equations that interrelate states in an arbitrarily large network is incompletely represented by a 2-unit model, owing to the limited number of nearest-neighbor interactions. Instead, a 4-unit model suffices to illustrate all the types of equations that relate the steady-state probabilities of arbitrary conformations to that of the all U state U...U (e.g., UU for 2-unit, UUUU for 4-unit model).

$$UBUU = K_c * [Ca^{2+}]_i * UUUU \quad (5a)$$

$$UB^*UU = K_b * (1 + f/g) * \gamma^p * UBUU, \quad p = 0 \quad (5b)$$

$$= K_b * (1 + f/g) * K_c * [Ca^{2+}]_i * UUUU \quad (5c)$$

$$UB^*BU = K_c * [Ca^{2+}]_i * UB^*UU \quad (5d)$$

$$= K_b * (1 + f/g) * K_c^2 * [Ca^{2+}]_i^2 * UUUU \quad (5e)$$

$$UB^*B^*U = K_b * (1 + f/g) * \gamma^p * UB^*BU, \quad p = 1 \quad (5f)$$

$$= K_b^2 * (1 + f/g)^2 * \gamma * K_c^2 * [Ca^{2+}]_i^2 * UUUU \quad (5g)$$

In Eq. 5b and 5f, p is not an additional parameter of the simulation, but a condition depicting the number of reactive (*) neighbors of the unit undergoing the transition. To minimize the resulting edge effects of using a finite number of RUs, the unit on each end of a linear array treats the unit at the opposite end as a neighbor. Hence, cooperative interactions affect each RU equally.

The second step is to sum all formulae like those in Eq. 5. The resultant expression accumulates the probabilities of all states and must therefore equal to unity. Because each term in the sum contains model parameters multiplied by U...U, the equation is trivially manipulated to express U...U in terms of model parameters. Substituting this explicit expression for U...U into expressions of the form in Eq. 5 yields the complete solution for the steady-state occupancy of all model states. Relative force (F/F_{max}) is specified by the weighted sum of the steady-state probabilities of all states in which the weighting factor is the number of reactive (force-generating) units in each state divided by L, the total number of RUs (e.g., 0 for UU, 0.5 for UB*, and 1 for B*B*). The calculation of F/F_{max} is repeated at 15 to 100 different values of $[Ca^{2+}]_i$ to simulate force-$[Ca^{2+}]_i$ curves (Fig. 12 *A* and *B*).

QUANTITATIVE MODEL RESULTS

Fig. 12 *A* shows the model results for control versus 1 μM isoproterenol; the solid lines show model predictions and the dotted lines indicate Hill curves with parameters averaged from fits to experimental data (Fig. 8). To fit the control data, we could adjust four independent parameters: K_c, γ, $K_a(1 + f/g)$, and $K_b(1 + f/g)$. Note that K_a, K_b, f, and

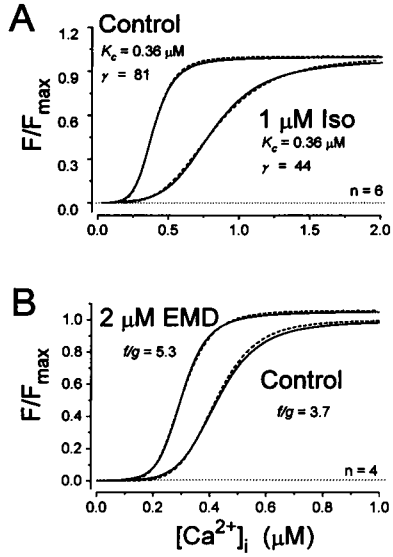

FIGURE 12 Model results, effects of 1 μM isoproterenol and 2 μM EMD. Results are best fit of model to average Hill curves as in Fig. 8 or Fig. 10. (*A*) Model results (*solid lines*) and Hill curves (*dotted lines*) for control versus 1 μM isoproterenol. The fits incorporate values of 0.1 for $K_b^*(1 + f/g)$ and 0.0001 for $K_a^*(1 + f/g)$, both for control and with isoproterenol. (*B*) Model results (*solid lines*) and Hill curves (*dotted lines*) for control versus 2 μM EMD. Parameter varied is f/g, the equilibrium constant for strong-binding cross-bridges. The model fits were generated by using the control values for K_a and K_b and assuming they did not change with EMD.

g cannot be determined individually because the equations for the network model invariably group these parameters together as specified in the third and fourth terms above. As a starting point for fitting control data, we bracketed K_c, the Ca^{2+} binding affinity to TnC, between experimentally determined values of 0.146 μM (Zot and Potter, 1987) and 0.4 μM (Tobacman and Sawyer, 1990). $K_a(1 + f/g)$ was initially set at 0.02, and $K_b(1 + f/g)$ was set at 0.2, to accord with data of cooperative myosin S-1 binding to thin filaments in skeletal muscle (McKillop and Geeves, 1991). γ was initially set at 5, in accordance with previous model analysis of skeletal muscle activation (Hill, 1983). These starting parameter values were then manually adjusted to provide an adequate fit to the control cardiac data. One set of satisfactory parameters is shown in the first row of Table 2, which gives rise to the solid curve relationship in Fig. 12 *A*, control. The main deviations from the initial parameter estimates are in $K_a(1 + f/g)$, and γ. $K_a(1 + f/g)$ had to be reduced to 0.0001 to prevent significant force development at resting $[Ca^{2+}]_i$ ($\approx$0.1 μM). The thin-filament, nearest-neighbor interaction term, γ, had to be increased to 81 to account for the far steeper force-$[Ca^{2+}]$ relations measured here in intact cardiac muscle instead of skinned skeletal muscle.

Turning now to the interpretation of isoproterenol effects, we reasoned that because F_{max} (which is proportional to $(1 + g/f)^{-1}$) was unchanged by isoproterenol, the ratio f/g must also be unchanged. To explain the experimentally observed decrease in cooperativity (Fig. 8), γ had to be reduced by 50%. Only by varying this parameter could the steepness of predicted force-$[Ca^{2+}]_i$ relations be altered sufficiently to account for the large experimental effect. No additional changes in the other parameters were required to account for the entire isoproterenol effect, including the experimentally observed increase in $K_{1/2}$. This excellent fit is demonstrated by the solid-curve model prediction in Fig. 12 *A* (isoproterenol), derived from the parameter set in the second row of Table 2. This simulation hints that reduction in nearest-neighbor cooperativity (γ) may be the primary mechanism by which isoproterenol alters the force-$[Ca^{2+}]_i$ relationship, without directly altering the TnC Ca^{2+} binding affinity. This differs in principle from the mechanism proposed by Robertson et al. (1982), by which phosphorylation of TnI affects myofilament Ca^{2+} sensitivity by increasing the off-rate for Ca^{2+} binding to TnC. However, a decrease in γ from 81 to 44 as proposed by our model will indirectly lead the network as a whole to manifest decreased Ca^{2+} binding affinity, shifting the $[Ca^{2+}]_i$ for 50% binding from 0.38 μM to 0.72 μM. Although it is widely accepted that β-adrenergic interventions such as isoproterenol lead to phosphorylation of a unique site on cardiac TnI (Solaro et al. 1976), the mechanism by which this phosphorylation alters thin filament regulation is still unknown. Holroyde et al. (1979) showed that phosphorylation by cAMP-dependent protein kinase leads to a decrease in the binding of Ca^{2+} to TnC in skinned myofibrils.

TABLE 2 Model parameters: effects of isoproterenol and EMD

	$K_a^*(1 + f/g)$	$K_b^*(1 + f/g)$	K_c (μM^{-1})	γ
Control	0.000100	0.100	0.36	81
Isoproterenol	0.000100	0.100	0.36	44
Control	0.000100	0.100	0.28	95
EMD	0.000136	0.136	0.28	95

Fig. 12 *B* shows the model analysis for control versus 2 μM EMD; again, the solid lines show the model results, and dotted lines indicate the corresponding Hill curves (from Fig. 10) generated by the experimentally determined, average Hill parameters. Because the Hill coefficient was not altered by EMD, the model cooperativity parameter γ was also not appreciably altered. The observed leftward shift in the force-$[Ca^{2+}]_i$ relationship (decreased $K_{1/2}$) could therefore be explained by either an increase in the Ca^{2+} binding affinity K_c (see Eq. 3b) or a change in cross-bridge kinetics, f/g (see Eq. 3a and c). However, a second constraint arises from the increase in F_{max}. Because F_{max} is proportional to $(1 + g/f)^{-1}$, this also suggests that f/g is altered. Could a single change in f/g explain both the leftward shift of the force-$[Ca^{2+}]_i$ relationship and the increase in F_{max}? Table 2 shows model parameter values that gave the best fit for control and EMD, respectively. With γ, K_a, K_b, and K_c unchanged, a simple increase in f/g by 45% sufficed to explain both observed effects of EMD. Increasing f/g causes little increase in Ca^{2+} bound to TnC. The $[Ca^{2+}]_i$ corresponding to half-maximal binding shifts minimally from 0.41–0.30 μM. Similarly, Solaro et al. (1993) found no appreciable increase in the total binding of Ca^{2+} to TnC with up to 30 μM EMD.

The model results are consistent with EMD causing an increase in affinity of strong-binding cross-bridges (Leijendekker and Herzig, 1992; Strauss et al., 1992; Solaro et al., 1993; Grob et al., 1993; Simnett et al., 1993). EMD increases force in TnI-depleted (Ca^{2+}-independent) skinned fibers (Strauss et al., 1992), further supporting a direct effect on cross-bridges rather than on steps involving Ca^{2+} regulation. If the increase in f/g causes the change in both $K_{1/2}$ and F_{max} (Table 2) as we have proposed (Fig. 12 *B*), there are sufficient experimental constraints to calculate f/g explicitly. The ratio of $K_a(1 + f/g)$ in EMD versus control (Table 2) that is required to fit the experimental effect can then be used to provide a first constraint:

$$1.36 = (1 + f/g)/(1 + f'/g'),$$

where the prime values refer to the EMD condition. The ratio of F_{max} in EMD and control (Fig. 10) constitutes a second constraint:

$$F'_{max}/F_{max} = 1.07 = (1 + g/f)/(1 + g'/f').$$

The two constraints permit us to conclude that f/g is 3.7 in the control and 5.3 with 2 μM EMD. We can then calculate the cross-bridge duty cycle ($1/(1 + g/f)$) to be 0.79 in control and 0.84 with EMD. These estimates are near the values of 0.7–0.8, determined from the ratio of active stiffness to rigor stiffness at F_{max} measured by Saeki et al. (1991).

DISCUSSION

Summary of experimental results

By hindering SR function with ryanodine to block phasic calcium release (Sutko and Willerson, 1980; Sutko et al., 1985) and with CPA to inhibit SR calcium uptake (Seidler et al., 1989), we were able to record force and $[Ca^{2+}]_i$ transients at very high $[Ca^{2+}]_o$. Because the SR no longer provided rapid removal of intracellular Ca^{2+}, the decline of the $[Ca^{2+}]_i$ transient (and therefore also the force transient) was greatly prolonged. In fact, the twitches were so slow that late relaxation force and $[Ca^{2+}]_i$ were in steady state. This was seen by superimposing force-$[Ca^{2+}]_i$ loops recorded at different $[Ca^{2+}]_o$ (Fig. 4 *A*). During late relaxation, force and calcium were defined by a unique relationship independent of contraction history.

Using this technique, we found that isoproterenol, a β-adrenergic agonist, caused both a rightward shift and a decrease in the steepness of the steady-state force-$[Ca^{2+}]_i$ relationship, as measured by an increase in $K_{1/2}$, the $[Ca^{2+}]_i$ that produces 50% of maximal tension, and by a decrease in the Hill coefficient n_H. In contrast, we found that EMD, an agent that is proposed to sensitize the myofilaments to calcium, caused a leftward shift in the force-$[Ca^{2+}]_i$ relationship as measured by a decrease in $K_{1/2}$, with no change in n_H. Unlike isoproterenol, which had no effect on the F_{max}, EMD caused an increase in F_{max}.

Appraisal of method for measuring steady-state force-$[Ca^{2+}]_i$

Most previous measurements of steady-state force-$[Ca^{2+}]_i$ relationships in intact muscle relied on the photoprotein aequorin to estimate $[Ca^{2+}]_i$. This technique has several drawbacks (see Blinks et al., 1982, for a review), which can be avoided by use of iontophoretically-loaded Fura-2 (Backx and ter Keurs, 1993). Our particular approach to determining steady-state force-$[Ca^{2+}]_i$ relationships in intact muscle offers several important advantages. During pharmacologically slowed relaxation, the $[Ca^{2+}]_i$ is changing slowly enough so as not to incur errors arising from potentially slow kinetics of the indicator Fura-2 in vivo (Baylor and Hollingworth, 1988). This limitation of Fura-2 may lead to underestimation of peak $[Ca^{2+}]_i$ during normal twitches (Blatter and Wier, 1990). In addition, multicellular preparations are most likely to behave uniformly during the slow declining phase (late during relaxation), when $[Ca^{2+}]_i$ is changing gradually.

A second advantage is that our method produces a continuous force-$[Ca^{2+}]_i$ relationship, with better resolution of the curve shape. Traditional protocols using skinned muscle usually obtain one force-$[Ca^{2+}]_i$ data point per solution $[Ca^{2+}]$. Likewise, tetanic stimulation produces only one data point per tetanus at different $[Ca^{2+}]_o$. To obtain similar resolution with tetanic stimulation would require such a large number of points that preparation rundown might preclude such an approach.

Third, our method provides excellent resolution in the low $[Ca^{2+}]_i$ range. Fura-2 provides very good resolution at low $[Ca^{2+}]_i$ (Grynkiewicz et al., 1985), in contrast to aequorin (Blinks et al., 1982). In addition, force-$[Ca^{2+}]_i$ curves measured during twitches at all $[Ca^{2+}]_o$ overlap at low $[Ca^{2+}]_i$, providing the greatest confirmation of the observed force-$[Ca^{2+}]_i$ relationship. Low $[Ca^{2+}]_i$ occurs at the tail end of twitch relaxation, where force and $[Ca^{2+}]_i$ are changing the most slowly and activation should be very uniform. In contrast, tetanization at submaximal calcium levels yields oscillations in both $[Ca^{2+}]_i$ and force (Yue et al., 1986). Thus there may be gradients of activation within the muscle that hinder the interpretation of the results.

Fourth, twitches are less likely than tetanic contractions to induce changes in intracellular pH and/or inorganic phosphate concentration. Changes in pH (Fabiato and Fabiato, 1978b) and inorganic phosphate (Kentish, 1986; Marban and Kusuoka, 1987) alter the force-$[Ca^{2+}]_i$ relationship. To reach a plateau of force and $[Ca^{2+}]_i$, the muscle may sometimes require tetanization for more than 2–3 s, by which time metabolic demands may shift the force-$[Ca^{2+}]_i$ relationship by the aforementioned mechanisms (Fig. 3 *A*). This scenario can result in an ambiguous tetanic force-$[Ca^{2+}]_i$ that depends on the time point chosen for measurement of force and $[Ca^{2+}]_i$ (Okazaki et al., 1990; Hongo et al., 1993). Our twitch method for gauging the steady-state force-$[Ca^{2+}]_i$ relationship can also suffer from analogous metabolic problems if contractions are not elicited at a sufficiently slow rate to ensure complete relaxation of mechanical activity between stimuli.

A possible limitation to our method would arise if either CPA or ryanodine alter myofilament calcium sensitivity. If so, the control force-$[Ca^{2+}]_i$ curves may already be shifted, although the qualitative changes seen with isoproterenol and EMD would still be valid. However, ryanodine has been shown not to alter the steady-state force-pCa relationship obtained in skinned muscle (Fabiato, 1985). Likewise, we found that the steady-state curve obtained in twitches with ryanodine alone did not differ from that obtained with both ryanodine and CPA, which supports the assertion that CPA does not alter myofilament calcium sensitivity. Using CPA (in addition to ryanodine) to prevent SR calcium uptake causes higher levels of $[Ca^{2+}]_i$ for a given level of $[Ca^{2+}]_o$.

This allows a greater portion of the force-calcium relationship to be measured.

Relationship to previous experimental results

The rightward shift and decreased slope of the steady-state force-calcium relationship we observed with isoproterenol provides a critical confirmation of previous results. Okazaki et al. (1990) showed similar effects with isoprenaline in ryanodine-tetanized ferret papillary muscles in which $[Ca^{2+}]_i$ was measured using aequorin. Similarly, they observed no change in F_{max}. However, the rightward shift that they observed has been difficult to interpret, given the technical limitations pertaining to the increasing phase of tetanic force-$[Ca^{2+}]_i$ relations (see above and Yue et al., 1986). Our results indicate that isoproterenol does indeed produce a rightward shift of the force-$[Ca^{2+}]_i$ relationship, most likely mediated through phosphorylation of TnI. We observed a similar rightward shift with 1 mM 8-bromo-cyclic AMP, arguing that cyclic-AMP-dependent kinase phosphorylation is the key modulatory event. This is in agreement with the results in skinned muscle, in which phosphorylation of TnI shifts the steady-state force-pCa relationship rightward (see Winegrad, 1984, for a review).

The leftward shift of the force-$[Ca^{2+}]_i$ relationship and the increase in F_{max} observed with EMD also agree with results obtained in skinned muscle. In fibers from both porcine ventricular muscle and failing human hearts, Beier et al. (1991) showed a similar decrease in the calcium required for half-maximal activation and an increase in the F_{max} produced by using EMD 53998. The positive enantiomer, EMD 57033, is believed to be responsible for the Ca^{2+}-sensitizing effects of EMD 53998, whereas the negative enantiomer, EMD 57439, is reported to have phosphodiesterase inhibitory activity (Gambassi et al., 1993; Lues et al., 1993). Using only the positive enantiomer, Grob et al. (1993) showed a leftward shift in the force-pCa relationship and an increase in F_{max} in skinned trabeculae from guinea pigs. In intact muscle, leftward shifts in the relationship between peak twitch force and peak amplitude of the aequorin transient were demonstrated (Lee and Allen, 1991); this effect has also been shown to be localized in the positive enantiomer EMD 57033 (White et al., 1993). Although not representing a steady-state relationship, those results are consistent with myofilament sensitization and the leftward shift of the steady-state force-$[Ca^{2+}]_i$ relationship demonstrated here.

Cooperative model of thin filament activation

Previous kinetic models of thin filament activation have used the proposal that seven actin monomers associated with a single tropomyosin molecule act as a cooperative unit (Tawada and Tawada, 1975; Hill et al., 1980; McKillop and Geeves, 1991). Our particular model formulation offers a number of advantages for interpretation of experimental results like those in this study. First, isometric force is an explicit output of our model, whereas previous models were developed to predict outcomes of biochemical assays such as myosin subfragment 1 binding isotherms. Second, our equations are formulated in a manner that facilitates numerical solution of steady-state behavior for large numbers of RUs linked by cooperative interactions. This is an important advantage, given the challenge of simulating experimentally determined force-$[Ca^{2+}]_i$ relationships with Hill coefficients near 6. In fact, solutions of 9 interacting RUs were required to obtain parameter estimates that were independent of the number of units (see above). Finally, our quantitative formulation articulates cooperative interactions in a conceptually obvious and explicit format that will facilitate calculation of nonsteady-state model behavior, such as would be required to predict the properties of physiological twitch contraction. For the sake of simplicity, in the present study we have made equilibrium assumptions to enable a simple numerical method for computation of steady-state behavior; however, the form of our equations lends itself to generalized solution by Monte Carlo simulation, without assumptions about either equilibrium or steady state.

Our model provides a concrete framework for assessment of different mechanisms that could modulate steady-state force-$[Ca^{2+}]_i$ curves with pharmacological and physiological intervention. The analysis emphasizes that modulation in the response between force and $[Ca^{2+}]_i$ is not limited to the one-dimensional interplay between sensitization and desensitization, but arises instead from a multidimensional balance among Ca^{2+} binding affinities, cooperative interactions, and cross-bridge kinetics. Quantitative models, together with continued refinement of experimental constraints including Ca^{2+} binding, may provide the specificity to distinguish definitively among the possibilities.

We thank Dr. M. Klockow, E. Merck Pharmaceuticals, for providing us with EMD 53998. We also thank Dr. Jon Peterson, Dr. Michael Berman, and Ms. Smadar Lapidot for their helpful comments on the manuscript. This work was supported by a National Science Foundation Presidential Faculty Fellowship (BCS-9253539) to D. T. Yue and by a Whitaker Foundation Award to the Department of Biomedical Engineering.

REFERENCES

Akahane, K., Y. Furukawa, Y. Ogiwara, M. Haniuda, and S. Chiba. 1989. Beta-2 adrenoceptor-mediated effects on sinus rate and atrial and ventricular contractility on isolated, blood-perfused dog heart preparations. *J. Pharmacol. Exp. Ther.* 248:1276–1282.

Backx, P. H., and H. E. D. J. ter Keurs. 1993. Fluorescent properties of rat cardiac trabeculae microinjected with Fura-2 salt. *Am. J. Physiol.* 264: H1098–H1110.

Baylor, S. M., and S. Hollingworth. 1988. Fura-2 calcium transients in frog skeletal muscle fibres. *J. Physiol.* 403:151–192.

Bean, B., M. Nowycky, and R. Tsien. 1984. β-Adrenergic modulation of calcium channels in frog ventricular heart cells. *Nature.* 307:371–375.

Beier, N., J. Harting, R. Jonas, M. Klockow, I. Lues, and G. Haeusler. 1991. The novel cardiotonic agent EMD 53998 is a potent "calcium sensitizer". *J. Cardiovasc. Pharmacol.* 18:17–27.

Blatter, L. A., and W. G. Wier. 1990. Intracellular diffusion, binding, and compartmentalization of the fluorescent calcium indicators indo-1 and Fura-2. *Biophys. J.* 58:1491–1499.

Blinks, J. R., W. G. Wier, P. Hess, and F. G. Prendergast. 1982. Measurement of Ca^{2+} concentrations in living cells. *Prog. Biophys. Mol. Biol.* 40:1–114.

Brandt, P. W., M. S. Diamond, and J. S. Rutchik. 1987. Cooperative interactions between troponin-tropomyosin units extend the length of the thin filament in skeletal muscle. *J. Mol. Biol.* 195:885–896.

Bremel, R. D., and A. Weber. 1972. Cooperation within actin filament in vertebrate skeletal muscle. *Nature New Biol.* 283:97–101.

Brenner, B. 1988. Effect of Ca^{2+} on cross-bridge turnover kinetics in skinned single rabbit psoas fibres: implications for regulation of muscle contraction. *Proc. Natl. Acad. Sci. USA.* 85:3265–3269.

Brown, A. M., D. L. Kunze, and A. Yatani. 1984. The agonist effect of dihydropyridines on Ca channels. *Nature.* 311:570–572.

de Tombe, P. P., and H. E. D. J. ter Keurs. 1990. Force and velocity of sarcomere shortening in trabeculae from rat heart. *Circ. Res.* 66: 1239–1254.

Dobrunz, L. E., P. H. Backx, and D. T. Yue. 1993. Steady-state calcium force relationship in intact twitching cardiac muscle: evidence for desensitization by isoproterenol. *Biophys. J.* 64:119*a*. (Abstr.)

Dobrunz, L. E., P. H. Backx, and D. T. Yue. 1994. Sensitizing agent EMD 53998 causes leftward shift of steady-state tension-$[Ca^{2+}]_i$ relationship in intact twitching cardiac muscle. *Biophys. J.* 66:318*a*. (Abstr.)

Fabiato, A. 1985. Effects of ryanodine in skinned cardiac cells. *Fed. Proc.* 44:2970–2976.

Fabiato, A., and F. Fabiato. 1978a. Myofilament-generated tension oscillations during partial calcium activation and activation dependence of sarcomere length-tension relation of skinned cardiac cells. *J. Gen. Physiol.* 72:667–699.

Fabiato, A., and F. Fabiato. 1978b. Effects of pH on the myofilaments and the sarcoplasmic reticulum of skinned cells from cardiac and skeletal muscle. *J. Physiol.* 276:233–255.

Gambassi, G., M. C. Capogrossi, M. Klockow, and E. G. Lakatta. 1993. Enantiomeric dissection of the effects of the inotropic agent, EMD 53998, in single cardiac myocytes. *Am. J. Physiol.* 264:H728–H738.

Gao, W. D., P. H. Backx, M. D. Azan-Backx, and E. Marban. 1994. Myofilament Ca^{2+} sensitivity in intact versus skinned rat ventricular muscle. *Circ. Res.* 74:408–415.

Grob, T., I. Lues, and J. Daut. 1993. A new cardiotonic drug reduces the energy cost of active tension in cardiac muscle. *J. Mol. Cell. Cardiol.* 25:239–244.

Grynkiewicz, G., M. Poenie, and R. Y. Tsien. 1985. A new generation of Ca^{2+} indicators with greatly improved fluorescent properties. *J. Biol. Chem.* 260:34440–34450.

Hill, T. L. 1983. Two elementary models for the regulation of skeletal muscle contraction by calcium. *Biophys. J.* 44:383–396.

Hill, T. L., E. Eisenberg, and L. Greene. 1980. Theoretical model for the cooperative equilibrium binding of myosin subfragment 1 to the actin-tropomyosin complex. *Proc. Natl. Acad. Sci. USA.* 77:3186–3190.

Holroyde, M. J., E. Howe, and R. J. Solaro. 1979. Modification of calcium requirements for activation of cardiac myofibrillar ATPase by cyclic AMP dependent phosphorylation. *Biochim. Biophys. Acta.* 586:63–69.

Hongo, K., E. Tanaka, and S. Kurihara. 1993. Alterations in contractile properties and Ca^{2+} transients by β- and muscarinic receptor stimulation in ferret myocardium. *J. Physiol.* 461:167–184.

Huxley, A. F. 1957. Muscle structure and theories of contraction. *Prog. Biophys. Mol. Biol.* 7:255–318.

Kentish, J. C. 1986. The effects of inorganic phosphate and creatine phosphate on force production in skinned muscles from rat ventricle. *J. Physiol.* 370:585–604.

Leavis, P. C., and J. Gergely. 1984. Thin filament proteins and thin-filament-linked regulation of vertebrate muscle contraction. *CRC Crit. Rev. Biochem.* 16:235–305.

Lee, J. A., and D. G. Allen. 1991. EMD 53998 sensitizes the contractile proteins to calcium in intact ferret ventricular muscle. *Circ. Res.* 69: 927–936.

Leijendekker, W. M., and J. W. Herzig. 1992. Reduction of myocardial cross-bridge turnover rate in presence of EMD 53998, a novel Ca^{2+}-sensitizing agent. *Pfluegers Arch.* 421:388–390.

Lues, I., N. Beier, R. Jonas, M. Klockow, and E. G. Lakatta. 1993. The two mechanisms of action of racemic cardiotonic EMD 53998 reside in different enantiomers. *J. Cardiovasc. Pharmacol.* 21:883–892.

Marban, E., and H. Kusuoka. 1987. Maximal Ca^{2+}-activated force and myofilament Ca^{2+} sensitivity in intact mammalian hearts. Differential effects of inorganic phosphate and hydrogen ions. *J. Gen. Physiol.* 90:609–623.

McKillop, D. F., and M. A. Geeves. 1991. Regulation of the acto-myosin subfragment 1 interaction by troponin/tropomyosin. *Biochem. J.* 279: 711–718.

Okazaki, O., N. Suda, K. Hongo, M. Konishi, and S. Kurihara. 1990. Modulation of Ca^{2+} transients and contractile properties by β-adrenoceptor stimulation in ferret ventricular muscles. *J. Physiol.* 423:221–240.

Puceat, M., O. Clement, P. Lechene, J. M. Pelosin, R. Ventura-Clapier, and G. Vassort. 1990. Neurohormonal control of calcium sensitivity of myofilaments in rat single heart cells. *Circ. Res.* 67:517–524.

Ray, K. P., and P. J. England. 1976. Phosphorylation of the inhibitory subunit of troponin and its effect on the calcium dependence of cardiac myofibril adenosine triphosphate. *FEBS Lett.* 70:11–16.

Robertson, S. P., J. D. Johnson, M. J. Holroyde, E. G. Kranias, J. D. Potter, and R. J. Solaro. 1982. The effect of troponin I phosphorylation on the Ca^{2+}-regulatory site of bovine cardiac troponin. *J. Biol. Chem.* 257: 260–263.

Saeki, Y., M. Kawai, and Y. Zhao. 1991. Comparison of crossbridge dynamics between intact and skinned myocardium from ferret right ventricles. *Circ. Res.* 68:772–781.

Seidler, N. W., I. Jona, M. Vegh, and A. Martonosi. 1989. Cyclopiazonic acid is a specific inhibitor of the Ca^{2+}-ATPase of sarcoplasmic reticulum. *J. Biol. Chem.* 264:17816–17823.

Simnett, S. J., S. Lipscomb, C. C. Ashley, and I. P. Mulligan. 1993. The effect of EMD 57033, a novel cardiotonic agent, on the relaxation of skinned cardiac and skeletal muscle produced by photolysis of diazo-2, a caged calcium chelator. *Pfluegers Arch.* 425:175–177.

Solaro, R. J., A. J. G. Moir, and S. V. Perry. 1976. Phosphorylation of TnI and the inotropic effect of adrenaline in the perfused rabbit heart. *Nature.* 262:615–616.

Solaro, R. J., G. Gambassi, D. M. Warshaw, M. R. Keller, H. A Spurgeon, N. Beier, and E. G. Lakatta. 1993. Stereoselective actions of thiadiazinones on canine cardiac myocytes and myofilaments. *Circ. Res.* 73:981–990.

Strauss, J. D., C. Zeugner, and J. C. Ruegg. 1992. The positive inotropic calcium sensitizer EMD 53998 antagonizes phosphate action on cross-bridges in cardiac skinned fibers. *Eur. J. Pharmacol.* 227:437–441.

Sutko, J. L., and J. T. Willerson. 1980. Ryanodine alteration of the contractile state of rat ventricular myocardium. *Circ. Res.* 46:332–343.

Sutko, J. L., K. Ito, and J. L. Kenyon. 1985. Ryanodine: a modifier of sarcoplasmic reticulum calcium release in striated muscle. *Fed. Proc.* 44:2984–2988.

Tada, M., and A. M. Katz. 1982. Phosphorylation of the sarcoplasmic reticulum and sarcolemma. *Annu. Rev. Physiol.* 44:401–423.

Tawada, Y., and T. Tawada. 1975. Co-operative regulation mechanism of muscle contraction: inter-tropomyosin co-operation model. *J. Theor. Biol.* 50:269–283.

ter Keurs, H. E., W. H. Rijnsburger, R. van Heuningen, and M. J. Nagelsmit. 1980. Tension development and sarcomere length in rat cardiac trabeculae. Evidence of length-dependent activation. *Circ. Res.* 46: 703–714.

Thomas, G., R. Grob, G. Pfitzer, and J. C. Ruegg. 1985. The positive inotropic dihydropyridine BAY K 8644 does not affect calcium sensitivity or calcium release of skinned cardiac fibres. *Naunyn-Schmiedebergs Arch. Pharmacol.* 328:378–381.

Tobacman, L. S., and D. Sawyer. 1990. Calcium binds cooperatively to the regulatory sites of the cardiac thin filament. *J. Biol. Chem.* 265:931–939.

Tsien, R. W. 1977. Cyclic AMP and contractile activity in heart. *Adv. Cyclic Nucleotide Res.* 8:363–420.

White, J., J. A. Lee, N. Shah, and C. H. Orchard. 1993. Differential effects of the optical isomers of EMD 53998 on contraction and cytoplasmic Ca^{2+} in isolated ferret cardiac muscle. *Circ. Res.* 73:61–70.

Winegrad, S. 1984. Regulation of cardiac contractile proteins. Correlations between physiology and biochemistry. *Circ. Res.* 55:565–574.

Yue, D. T., E. Marban, and W. G. Wier. 1986. Relationship between force and intracellular $[Ca^{2+}]$ in tetanized mammalian heart muscle. *J. Gen. Physiol.* 87:223–242.

Zot, H. G., and J. D. Potter. 1987. Calcium binding and fluorescence measurements of dansylaziridine-labelled troponin C in reconstituted thin filaments. *J. Muscle Res. Cell Motil.* 8:428–436.